Journal of the European Ceramic Society **12** (1993) 61–69

Crystallization Characteristics of Iron-Containing Spodumene–Diopside Glasses

Samia N. Salama & S. M. Salman

Glass Research Department, National Research Centre, Dokki, Cairo, Egypt

(Received 7 August 1992; revised version received 6 January 1993; accepted 1 February 1993)

Abstract

The crystallization characteristics of glasses based on a stoichiometric spodumene ($LiAlSi_2O_6$)–diopside ($CaMgSi_2O_6$) composition with addition of Fe_2O_3 replacing Al_2O_3 are described. The effects of compositional variation due to the Al_2O_3/Fe_2O_3 replacement and thermal treatment on the nature, type and stability fields of crystallizing phases as well as the resulting microstructure are traced by DTA, X-ray diffraction (XRD) and scanning electron microscopy (SEM).

In most cases, intense uniform bulk crystallization with fine-grained microstructure were achieved on increase of iron oxide at the expense of alumina. The crystallizing phases, β-eucryptite solid solution (ss), β-spodumene ss, varieties of pyroxene solid solution of diopside, hedenbergite and augite nature are mostly formed together, in some cases, with α-quartz, lithium silicates, lithium ferrate ($LiFeO_2$) and iron oxide. The type, stability and compatibility of the crystallized phases are discussed in relation to the compositional variation of the glass and thermal treatment.

Kristallisationscharakteristika von Gläsern auf der Basis von stöchiometrischen Spodumen ($LiAlSi_2O_6$)-Diopsid ($CaMgSi_2O_6$)-Zusammensetzungen mit zusätzlichem Fe_2O_3, das Al_2O_3 ersetzt, werden beschrieben. Die Auswirkungen der Zusammensetzungsänderung verursacht durch Al_2O_3/Fe_2O_3-Austausch und Wärmebehandlung auf sowohl Art, Typ und Stabilitätsbereiche der kristallisierenden Phasen als auch auf die resultierende Mikrostruktur werden mit DTA, Röntgenbeugung (XRD) und Rasterelektronenmikroskopie (SEM) nachgeprüft.

In den meisten Fällen wurde mit Zunahme von Eisenoxid anstelle von Aluminiumoxid starke und gleichmäßige Kristallisation mit feinkörniger Mikrostruktur erreicht. Die kristallisierenden Phasen β-Eukryptit-Mischkristalle (ss), β-Spodumen (ss) und Varietäten von Pyroxen-Mischkristallen aus Diopsid, Hedenbergit und Augit werden meistens zusammen gebildet, manchmal mit α-Quartz, Lithiumsilikaten, Lithium-ferraten ($LiFeO_2$) und Eisenoxid. Typ, Stabilität und Kompabilität der kristallisierten Phasen werden in Zusammenhang mit Änderungen der Zusammensetzung des Glases und Wärmebehandlung diskutiert.

On décrit les caractéristiques de cristallisation de verres à base de compositions stoechiométriques de spodumène ($LiAlSi_2O_6$) et de diopside ($CaMgSi_2O_6$) dans lesquels des ajouts de FeO_3 remplacent Al_2O_3. Les effets de ces variations de composition consistant en des substitutions Al_2O_3/Fe_2O_3, ainsi que des traitements thermiques, sur la nature, le type et les domaines de stabilité des phases cristallisées et sur les microstructures résultantes sont suivis par DTA, diffraction des RX (XRD) et microscopie électronique à balayage (SEM).

Dans la plupart des cas, une cristallisation uniforme et intense de la masse avec une microstructure fine est obtenue en augmentant la teneur en Fe_2O_3 au détriment de celle en Al_2O_3. Les phases qui cristallisent, à savoir β-eucryptite solution solide (ss), β-spodumène ss, solutions solides de pyroxène formées de diopside, hedenbergite et augite, sont le plus souvent formées ensemble avec, dans certains cas, du quartz α, des silicates de lithium, ferrates de lithium ($LiFeO_2$) et de l'oxyde de fer. La nature, la stabilité et la compatibilité des phases cristallines sont discutées en fonction des variations de composition du verre et du traitement thermique appliqué.

1 Introduction

The behaviour of iron-containing oxide glasses with heat-treatment to form glass-ceramics has been a subject of considerable importance, especially in

Journal of the European Ceramic Society 0955-2219/93/$6.00

determining the magnetic, electric and other properties of the resultant materials.[1] If iron-containing phases and the related solid solution could be crystallized in a controlled way from an iron-rich glass composition, it could offer a unique method for the control of the magnetic and electrical properties of the resultant material.[2]

Glass compositions crystallizing to give solid solutions should be of importance from the point of view of the physical properties of the material.[3] Because of the unique properties of lithium aluminosilicate, β-eucryptite and β-spodumene solid solution (ss) i.e. low thermal expansivity and exceptional chemical durability, glass-ceramics based on these phases are the most important from the standpoint of technical use.[4] The casting properties of the glass-ceramics are also improved by the presence of a high content of pyroxene phases. An increase of pyroxene content is most desirable as it constitutes the mineral phases which improve the abrasion resistance, the mechanical strength and the chemical properties of the material.[5] Minerals capable of wide isomorphous substitution in their crystal structure and having the necessary physical and chemical characteristics, such as lithium aluminosilicate and pyroxenes, may form the basis for production of many crystalline and glass-ceramic materials.

Work dealing with crystallization characteristics and phase relation in either iron pyroxenes or aluminosilicate glasses has been reported extensively;[5,6] however, work relating spodumene and pyroxene to each other, especially in the presence of high iron oxide content, has received little attention. In this paper a study of the effect of Fe_2O_3/Al_2O_3 replacement on the nucleation, crystallization characteristics, phase assemblages and extent of solid solution of glasses of stoichiometric spodumene–diopside composition is reported. The purpose of this study is to determine something about the role played by iron oxide in the resultant glasses and to examine the crystallization products and to relate this information back to information about the glass.

2 Experimental

2.1 Glass composition and preparation

Seven glass compositions based on an equimolar ratio of stoichiometric spodumene ($LiAlSi_2O_6$)–diopside ($CaMgSi_2O_6$), with partial replacement of Al_2O_3 by Fe_2O_3, were selected for the present investigation. Details of the glass oxide constituents are given in Table 1. Acid-washed pulverized quartz sand, and Analar grade Li_2CO_3, $CaCO_3$, $MgCO_3$, ferric oxide (red and anhydrous) and Al_2O_3 were used as starting materials. The weighed batch materials were thoroughly mixed and the glass was made by fusing the batch material in Pt–2% Rh crucibles in an electric furnace with SiC heating element at 1400°C for 3 h. The homogeneity of the melt was achieved by swirling the melt-containing crucible several times at about 20 min intervals. The melt was cast into rods and as buttons which were then properly annealed in a muffle furnace to minimize the strain.

2.2 Differential thermal analysis

The thermal behaviour of the powder glass samples (−100 mesh) was examined using a Shimadzu DT-30 differential thermoanalyser. The powdered sample was heated in a Pt holder against another Pt holder containing Al_2O_3 as a standard material. A heating rate of 20°C/min and a sensitivity setting of 20 μv/in were maintained for all the runs.

2.3 Thermal treatment

The crystallization process was investigated using both single- and double-stage heat-treatment regimes. The glass samples were first heated, according to the DTA results, at the endothermic

Table 1. Composition of the glasses

Glass number	*Oxide components*											
	mol%						*wt%*					
	Li_2O	*CaO*	*MgO*	*Fe_2O_3*	*Al_2O_3*	*SiO_2*	*Li_2O*	*CaO*	*MgO*	*Fe_2O_3*	*Al_2O_3*	*SiO_2*
Spodumene—diopside base glass												
G_1	7·14	14·26	14·26	—	7·14	57·20	3·71	13·95	10·02	—	12·66	59·66
Iron glasses												
G_2	7·14	14·26	14·26	1	6·14	57·20	3·67	13·77	9·89	2·75	10·78	59·14
G_3	7·14	14·26	14·26	2	5·14	57·20	3·64	13·63	9·79	5·45	8·93	58·56
G_4	7·14	14·26	14·26	3	4·14	57·20	3·60	13·50	9·70	8·10	7·12	57·98
G_5	7·14	14·26	14·26	4	3·14	57·20	3·57	13·37	9·61	10·68	5·35	57·42
G_6	7·14	14·26	14·26	6	1·14	57·20	3·50	13·11	9·43	15·72	1·91	56·33
G_7	7·14	14·26	14·26	7·14	—	57·20	3·46	12·97	9·33	18·51	—	55·73

peak temperature for 3 h, which was followed by another treatment at the exothermic peak temperature for 5 h. In some cases, however, the glasses were heated at 950°C and the duration was extended to 10 h.

2.4 Material investigation

To investigate the crystallizing samples, the powder X-ray diffraction patterns were obtained using a Phillips-type diffractometer with Ni-filtered Cu radiation. The crystallization characteristics and internal microstructures of the resultant material were examined on the fractured surfaces of the samples by scanning electron microscopy (SEM), where representative electron micrographs were obtained using a Semco Nanolab 7 scanning electron microscope.

3 Results

3.1 Differential thermal analysis

The DTA traces of the glasses (Fig. 1) showed endothermic effects in the 625–650°C temperature range. These endothermic effects are to be attributed to the glass transition, at which the atoms begin to arrange themselves in preliminary structural elements subsequent to crystallization. Various exothermic effects in the 780–870°C temperature range, indicating crystallization reaction in the glasses, are also recorded. The endothermic dip as well as the onset of crystallization were shifted to lower temperature with additions of Fe_2O_3 instead of Al_2O_3.

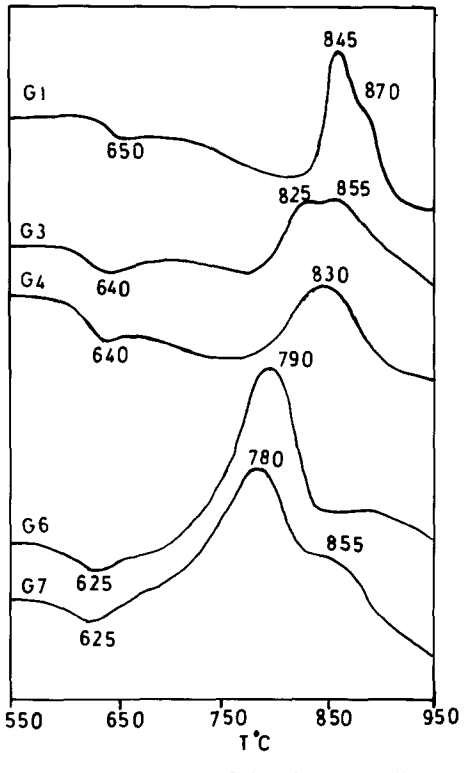

Fig. 1. DTA curves of the glasses studied.

3.2 Appearance of the crystallized glass

All the iron-containing glasses changed colour upon heating. The glasses of 2 mol% Fe_2O_3 turned medium olive green, the glass of 3 mol% Fe_2O_3 turned greyish green in bulk and was yellow on the surface, while for 4 mol% iron oxide the bulk of the glass turned deep greyish green. As the iron content was increased, the bulk of the glass turned a deep fine greyish colour and was a deep brown colour on the surface.

3.3 Crystallization characteristics

The presence of Fe_2O_3 stimulated the crystallization in the glass during heat-treatment. The glassy matrix was markedly decreased with addition of Fe_2O_3 at the expense of Al_2O_3. Fe_2O_3 remarkably decreased the temperature at which the crystallization starts. DTA (Fig. 1) revealed that the temperature of the endotherms of the glasses decreased by addition of iron oxide instead of Al_2O_3, i.e. a lower energy is needed to induce crystallization in such glasses. SEM micrographs of fractured surfaces of the crystallizing glasses with different Fe_2O_3/Al_2O_3 ratios are presented in Figs 2–5. All the Fe_2O_3-containing samples with >2 mol% Fe_2O_3 show reasonably uniform microstructure. The micrographs show the effect of addition of iron oxide (instead of Al_2O_3) on crystal growth and/or nucleation where the mean average of the crystal size of the glasses of 4–6 mol% Fe_2O_3 is around 4·8–1·7 μm. Iron oxide acts as a crystallization catalyst, accelerates the crystallization process and increases the rate of nucleation. G_6 (with high Fe_2O_3 content) shows numerous prismatic crystals or tiny aggregates greater in number than in G_5 (with lower Fe_2O_3 content) (Figs 4 and 5).

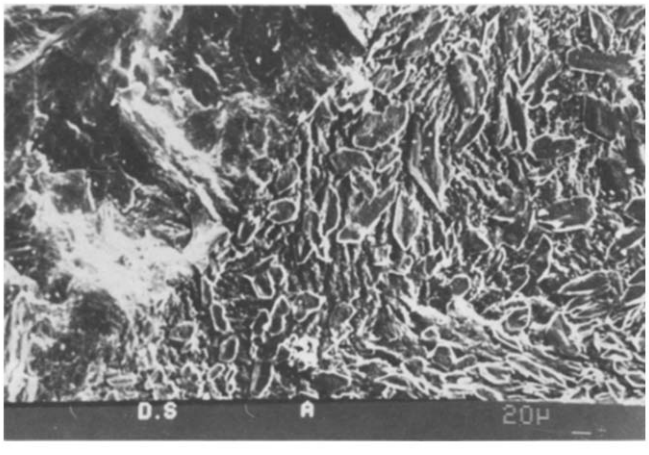

Fig. 2. SEM micrograph of fractured surface of iron oxide-free glass (G_1) crystallized at 650°C/3 h, 900°C/5 h, showing the hexagonal β-eucryptite and tetragonal β-spodumene together with fibrous diopside phase (bar = 20 μm).

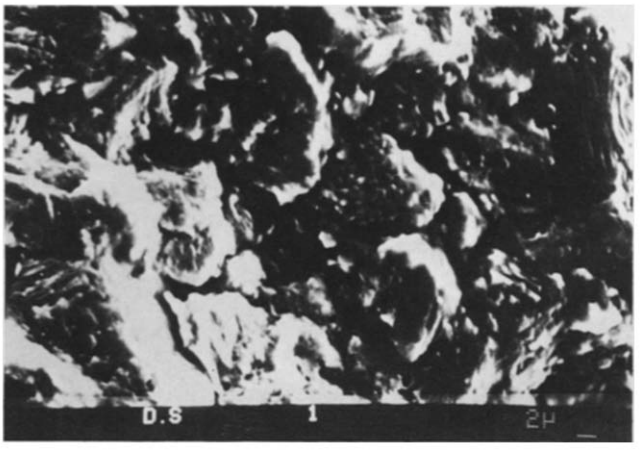

Fig. 3. SEM micrograph of fractured surface of G_3 (with 2 mol% Fe_2O_3), crystallized at 640°C/3 h, 950°C/10 h, showing rounded-like growths of β-spodumene and fibrous pyroxene phases (bar = 2 μm).

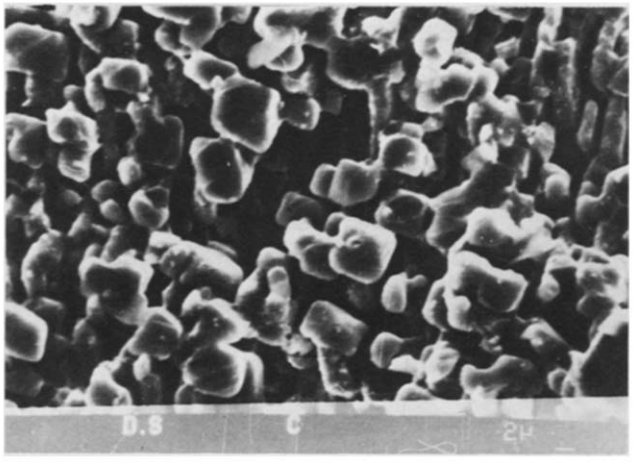

Fig. 4. SEM micrograph of fractured surface of G_5 (with 4 mol% Fe_2O_3), crystallized at 625°C/3 h, 950°C/10 h, showing uniform microstructure of numerous hedenbergite ss and β-spodumene crystals (bar = 2 μm).

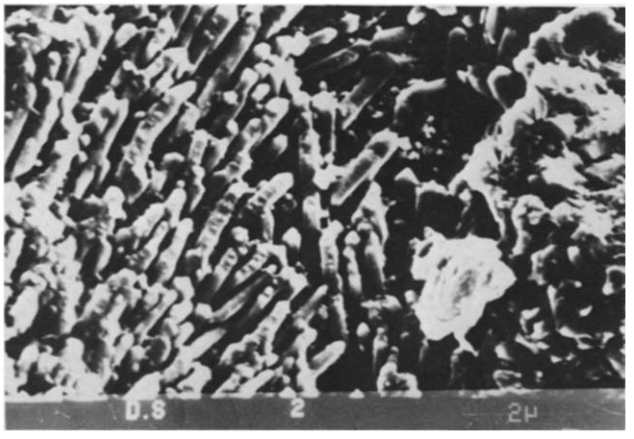

Fig. 5. SEM micrograph of fractured surface of G_6 (with 6 mol% Fe_2O_3), crystallized at 625°C/3 h, 800°C/5 h, showing numerous prismatic-like growths of augite pyroxene ss crystals (bar = 2 μm).

3.4 Crystallizing phases and solid solution developed

The phases developed in the glasses over the investigated 700–950°C temperature range as identified by the X-ray analysis (Figs 6–8, Table 2), were lithium-bearing phases β-eucryptite ss, β-spodumene ss, and varieties of iron pyroxene solid solution of diopside, hedenbergite and augite nature. In some cases, however, especially in the high Fe_2O_3-containing glass ($\geq 6\%$), α-quartz, lithium silicate, lithium ferrate ($LiFeO_2$) and iron oxide were also encountered. Neither any crystalline $LiFeSi_2O_6$ modification nor ferrite ($LiFe_5O_8$) phases were found among the crystallization products. The type and proportions of the resulting crystalline phases were determined mainly by the extent of Fe_2O_3/Al_2O_3 replacement in the glass and the crystallization parameters.

In general, as the alumina content of the glass was decreased (i.e. iron oxide increased), the amount of β-

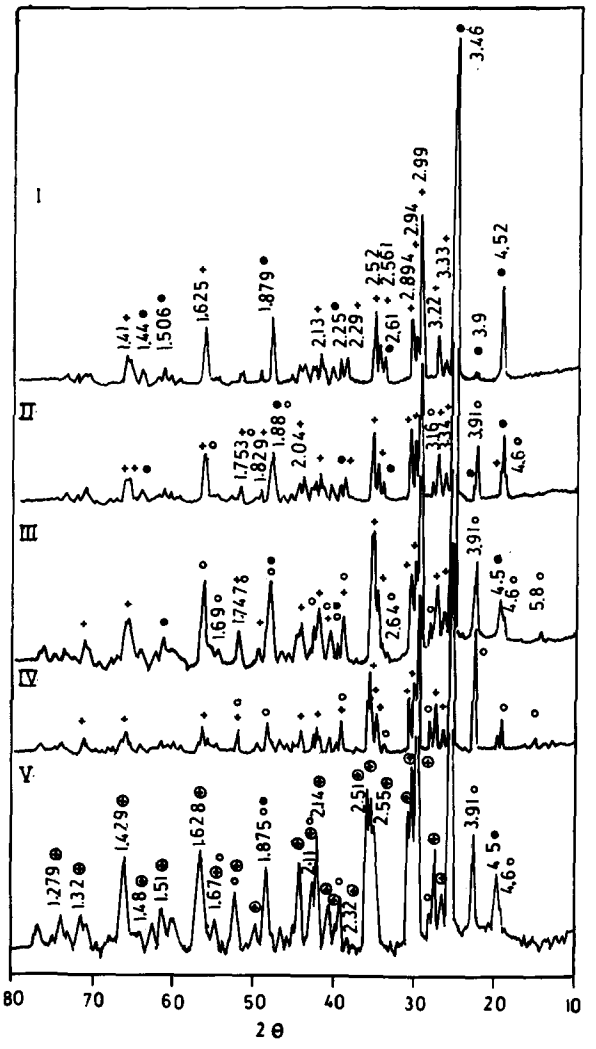

Fig. 6. XRD of various iron oxide glasses crystallized at different temperatures. I—G_1, 650°C/3 h, 840°C/5 h; II—G_1, 650°C/3 h, 900°C/5 h; III—G_2, 650°C/3 h, 840°C/5 h; IV—G_2, 650°C/3 h, 900°C/5 h; V—G_4, 640°C/3 h, 830°C/5 h. ●, β-eucryptite ss; ○, β-spodumene ss; +, diopside; ⊕, hedenbergite ss.

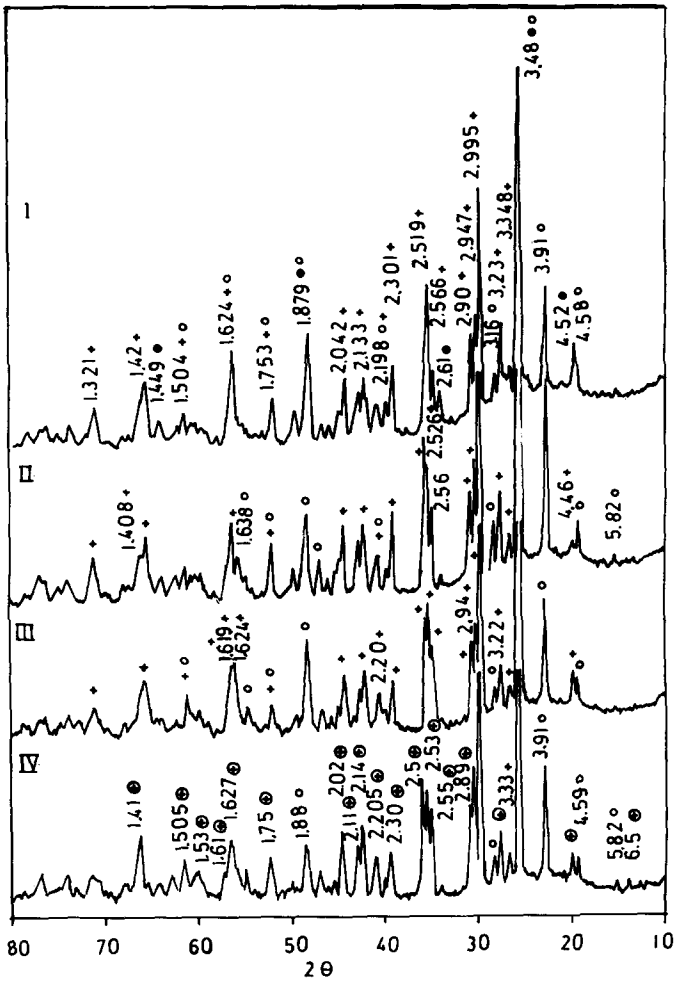

Fig. 7. XRD of various iron oxide glasses crystallized at 650°C/3 h, 950°C/10 h. I—G_1; II—G_2; III—G_3; IV—G_4. ●, β-eucryptite ss; ○, β-spodumene ss; +, diopside; ⊕, diopsidic hedenbergite ss.

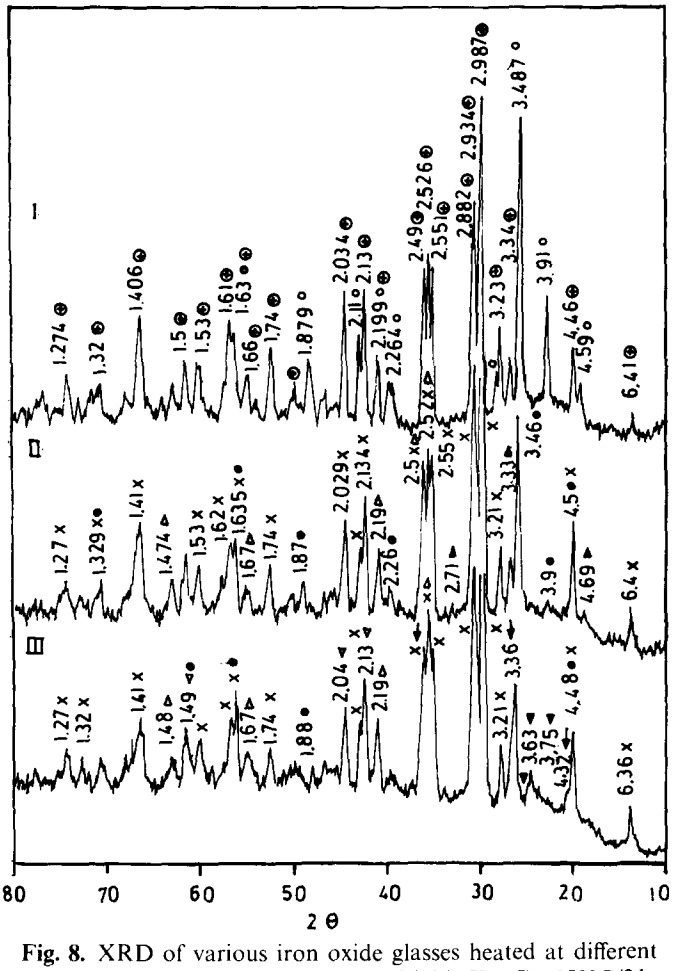

Fig. 8. XRD of various iron oxide glasses heated at different temperatures. I—G_5, 650°C/3 h, 950°C/10 h; II—G_6, 650°C/3 h, 800°C/5 h; III—G_7, 650°C/3 h, 850°C/5 h. ●, β-eucryptite ss; ○, β-spodumene ss; ⊕, hedenbergite ss; ×, augite ss; ↓, α-quartz; ▽, β-$LiFeO_2$; △, Fe_2O_3; ▲, Li_2SiO_3; ▼, $Li_2Si_2O_5$.

eucryptite or β-spodumene was decreased, while that of the pyroxene phase was increased. The phases are crystallized in the following sequence during stepwise heat-treatment. At low temperatures, the crystallization began with a β-eucryptite ss phase which immediately followed by the crystallization of iron pyroxene phases. Irreversible transformation of the initially formed β-eucryptite ss into β-spodumene took place at about 900°C in iron-free glass (i.e. G_1). The transformation temperature was steadily decreased with addition of iron oxide instead of Al_2O_3. For iron oxide-free glass (i.e. G_1) the X-ray analysis (Fig. 6, XRD pattern I) revealed that typical *d*-spacing lines of diopside (lines 3.33, 3.22, 2.99, 2.94, 2.894, 2.56, 2.52), together with β-eucryptite ss (lines 4.52, 3·46, 2·61, 1·879) were only detected by crystallization around the first exothermic temperature (840°C). β-Spodumene ss (lines 4.6, 3.91, 3.47, 3.16) was developed as well by the crystallization of G_1 near the second exothermic temperature, i.e. 900°C (Fig. 6, XRD pattern II) or at 950°C (Fig. 7, XRD pattern I).

At low Fe_2O_3 addition instead of Al_2O_3 (i.e. 1 mol% Fe_2O_3) G_2 heated to 840°C developed β-spodumene, β-eucryptite and diopside (Fig. 6, XRD pattern III); at higher temperature (i.e. 900°C or more) only β-spodumene and diopside were encountered (Fig. 6, XRD pattern IV and Fig. 7, XRD pattern II). On increasing the iron oxide replacement for Al_2O_3 up to 2 mol% Fe_2O_3 i.e. in G_3, iron-containing pyroxene of diopsidic type (Table 2) was formed together with β-eucryptite by heating the glass around the first exothermic temperature (i.e. 825°C). At the second exothermic temperature, 860°C or 950°C, β-spodumene ss was formed instead of β-eucryptite (Fig. 7, XRD pattern III).

For the glass with 3 mol% Fe_2O_3 replacing Al_2O_3, i.e. G_4, the X-ray analysis (Fig. 6, XRD pattern V) of the glass treated at the exothermic reaction temperature (830°C) clearly showed the *d*-spacing lines close to diopsidic hedenbergite solid solution (lines 3.33, 3.22, 2.99, 2.95, 2.89, 2.55, 2.53, 2.51, 2.14, 2.11, 1.627), β-spodumene ss and β-eucryptite. At higher temperature only β-spodumene ss together with the iron pyroxene ss were developed (Fig. 7, XRD pattern IV). Pyroxene solid solution of hedenbergite type was also developed in G_5 (with 4 mol% Fe_2O_3) together with the lithium aluminosilicate solid solution (β-eucryptite and/or

Table 2. The crystalline phases developed in the glasses of various iron oxide content

Glass number	*Molar ratios*		*Heat-treatment (°C/h)*	*Phases developed*
	Li_2O/Al_2O_3	Fe_2O_3/Al_2O_3		
G_1	1	Free of iron	800/5	β-Eucryptite ss, diopside
			650/3, 840/5	β-Eucryptite ss, diopside
			650/3, 900/5	β-Eucryptite ss, diopside, β-spodumene ss (minor)
			650/3, 950/10	β-Spodumene ss, diopside, β-eucryptite ss (minor)
G_2	1·16	0·16	800/5	β-Eucryptite ss, diopside
			650/3, 840/5	β-Spodumene ss, β-eucryptite ss, diopside
			650/3, 900/5	β-Spodumene ss, diopside
			650/3, 950/10	β-Spodumene ss, diopside
G_3	1·40	0·39	800/5	β-Eucryptite ss, diopsidic pyroxene ss
			640/3, 825/5	β-Eucryptite ss, diopsidic pyroxene ss
			640/3, 860/5	β-Spodumene ss, diopsidic pyroxene ss
			640/3, 950/10	β-Spodumene ss, diopsidic pyroxene ss
G_4	1·72	0·72	750/5	β-Eucryptite ss, diopsidic hedenbergite ss
			640/3, 830/5	β-Spodumene ss, hedenbergite ss, β-eucryptite ss (minor)
			640/3, 950/10	β-Spodumene ss, hedenbergite ss
G_5	2·27	1·27	750/5	Hedenbergite ss, β-eucryptite ss
			625/3, 800/5	Hedenbergite ss, β-spodumene ss, β-eucryptite ss
			625/3, 950/10	Hedenbergite ss, β-spodumene ss
G_6	6·26	5·26	700/5	Augitic pyroxene ss, β-eucryptite
			625/3, 750/3	Augitic pyroxene, β-eucryptite ss
			625/3, 800/5	Augitic pyroxene ss, β-eucryptite, Li_2SiO_3, Fe_2O_3
G_7	Free of Al_2O_3		700/5	Augitic pyroxene ss, α-quartz, $Li_2Si_2O_5$, β-$LiFeO_2$, Fe_2O_3
			625/3, 780/5	Augitic pyroxene ss, α-quartz, $Li_2Si_2O_5$, β-$LiFeO_2$, Fe_2O_3
			625/3, 855/5	Augitic pyroxene ss, α-quartz, $Li_2Si_2O_5$, β-$LiFeO_2$, Fe_2O_3

β-spodumene ss); at 750°C β-eucryptite was developed, while at 850°C or more β-spodumene crystallized as well (Fig. 8, XRD pattern I).

The glass with higher Fe_2O_3/Al_2O_3 replacement, i.e. 6 mol% Fe_2O_3, G_6, developed iron-containing pyroxenes together with lithium aluminosilicate, lithium metasilicate and iron oxide. The X-ray analysis (Fig. 8, XRD pattern II) revealed that the crystallization of G_6 around the exothermic temperature (790°C) developed augite pyroxene ss (lines 6.4, 4.5, 2.98, 2.55, 2.52, 2.13, 2.029), β-eucryptite, Li_2SiO_3 (lines 4.69, 3.33, 2.71) and Fe_2O_3 (lines 2.5, 2.19, 1.67, 1.74).

For the glass based on the Li_2O–CaO–MgO–Fe_2O_3–SiO_2 composition, i.e. G_7, the X-ray analysis (Table 2 and Fig. 8, XRD pattern III) indicated that the crystallization according to the DTA results (i.e. at 780°C) or at higher temperature (850°C) generally developed predominantly augite pyroxene ss (lines 6.36, 4.48, 3.21, 2.98, 2.55, 2.13), α-quartz (lines 4.32, 3.36, 2.5) with some lithium ferrate ($LiFeO_2$) (lines 2.13, 2.04, 1.49), lithium disilicate (lines 3.75, 3.63) and residual iron oxide (Fig. 8, XRD pattern III).

4 Discussion

Transition metal oxides like iron oxide are known to affect both nucleation and crystallization of silicate glass.[3,7] The presence of Fe_2O_3 even in small amounts has a considerable influence on the crystallizability and nucleation of the glass during the heating process. Williamson *et al.*[8] found that the crystal growth rates were dependent not only on the amount of iron oxide added to the glass but also on the ferrous (Fe″)/ferric (Fe‴) ratio of the iron in the glass. Rogers[3] and Williamson[9] noticed that only those glasses containing 5 mol% or more iron oxide present mainly in the ferric state showed any tendency to nucleate internally. They indicated also that a spinel phase was the first detectable phase that has been crystallized and they concluded that the main role in catalysing the silicate glasses appears to be that of enhancing the ability of spinel nuclei to form.

The change in nucleation rate is indicated by increasing the crystallization centres in the glass, as shown by SEM of the samples with different iron content nucleated for identical time, and is evidence that iron oxide favours nucleation. By scanning electron microscopy it is clear that a large number of crystals and tiny growths are always found in the high iron content samples. This is attributed to the fact that the iron is able to change its valence in glass matrix;[10,11] a transfer of valence electrons between the ions can create regions of local energy difference, thus accelerating the nuclei formation. In addition, the iron atom differs from the ion it replaces both in radius and force constants, and structural defects corresponding to the composition of the solid solution could be formed or be concomitant. Vacancies and a distorted framework with weakened energy bond may be created, both effects leading to enhanced diffusion rates.[11] This explains the ease

of the crystallization process of the glasses in which Fe_2O_3 was added at the expense of Al_2O_3.

In the present work the resulting crystalline phases formed, namely the lithia alumina-bearing phases (β-eucryptite ss and β-spodumene ss) and iron pyroxene phases, were mainly determined by the composition of the base glass and the degree of equilibria of the mineral-forming process. On addition of iron oxide (Fe_2O_3) at the expense of Al_2O_3 in the glasses of stoichiometric spodumene–diopside composition the β-eucryptite and/or β-spodumene were decreased while the pyroxene phases were increased. The development of *d*-spacing reflections (e.g. 2.98, 2.934, 2.55, 2.52, 2.50) and displacement of the major characteristic *d*-spacing lines of the pyroxene variety towards higher 2θ values may support the suggestion that the iron oxide (Fe‴ and/or Fe″) was incorporated in the iron pyroxene solid-solution phases; diopside, hedenbergite and/or augite. No displacement was observed in the main characteristic lines of β-eucryptite and/or β-spodumene, indicating the inclusion of iron oxide in the pyroxene structure.

The occurrence of β-eucryptite ss (β-quartz structured phase) and β-spodumene ss (keatite structured phase)[12] was essentially a function of the crystallization parameters applied and the composition of the glass of variable Fe_2O_3/Al_2O_3 ratio. Thus the lithium aluminosilicate phase developed at low temperature (700–850°C) in the glasses of relatively low Fe_2O_3/Al_2O_3 ratio (e.g. G_1 and G_2) was a metastable β-quartz structured phase, wherein the Si^{4+} were replaced by Al^{3+} in pairs with Li^+ ions,[12,13] and this phase recrystallized entirely into the stable β-spodumene ss at temperature above either 800 or 900°C, depending upon the Fe_2O_3/Al_2O_3 ratio present in the glasses.

β-Eucryptite ss is the phase most likely to be formed first, even from glasses of stoichiometric spodumene composition, due to the fact that the symmetry of the hexagonal β-eucryptite lattice is closer to the spherically symmetric glass structure than that of the tetragonal β-spodumene.[14] The SEM clearly showed the formation of both hexagonal β-eucryptite and the tetragonal β-spodumene in the iron-free glass heated at 900°C (Fig. 2). The persistence of β-eucryptite to such a high temperature (900°C in the case of G_1) conforms with the findings of Ray & Muchaw[12] for Li_2O–MgO–Al_2O_3–$nSiO_2$ glasses, where the high quartz ss phases developed at relatively low temperature were not transformed at high temperature into keatite ss (β-spodumene ss) when *n* was less than 3·5. On the other hand, the β-eucryptite ss–β-spodumene ss transformation is accelerated with addition of iron oxide in the glass at the expense of Al_2O_3. This may be attributed to the well-known effect of Fe_2O_3 in reducing the viscosity of the melt and glasses (as compared to Al_2O_3),[8] a condition which weakens the structural bond and facilitates the mobility and diffusion of the ions in the glass, thus enhancing the β-eucryptite–β-spodumene transformation.

Pyroxene consists of a group of minerals of variable composition which crystallize fairly readily. They are closely related in crystallographic and other physical properties, as well as in chemical composition.[15] A wide variety of ionic substitution occurs in the members of the pyroxene group, and there is complete replacement between some of the group components,[15] e.g. between diopside ($CaMgSi_2O_6$) and hedenbergite ($CaFe''Si_2O_6$). Furthermore, the diopside–hedenbergite minerals form a continuous chemical series with augite and ferroaugite ($(CaMgFe'')SiO_3$). The complexity of this group is exhibited by the wide isomorphism of the various elements in the expandable pyroxene formula:[16] $W_{1-p}(X, Y)_{1+p}Z_2O_6$ where W = Ca, Na; X = Mg, Fe″, Mn, Zn, Li; Y = Al, Fe‴, Cr, Ti, Z = Si, Al, Fe‴, and p = number of ions.

The wide range of replacement in the (X, Y) group commonly involving substitution of ions of different charge necessitates compensatory replacement in either the W or Z group, and the replacement must be such that the sum of the charges in the W, X, Y and Z group is 12.

Iron oxide can be present in the glass as ferrous (Fe″) and ferric (Fe‴) ions, and their ratio depends upon the glass composition and melting conditions. In silicate glasses, the ferric cation may occupy octahedral FeO_6 and tetrahedral FeO_4 sites,[10] while the ferrous cations occupy only octahedral sites which decrease by increasing the iron content.[17] The presence of an appreciable amount of Li_2O together with Fe_2O_3 in the present glasses greatly favours the formation of non-bridging oxygen atoms. The high concentration of non-bridging oxygen in silicate glass will favour Fe″ in the network-forming position as $Fe''O_4$.[18] As the number of non-bridging oxygen atoms is greatly increased, the Fe″ ions are oxidized to Fe‴, a large percentage of which would favour the network-forming position as $Fe'''O_4$.

Since high alkali concentration increases the ferric–ferrous ratios,[19] it is believed that $LiFe'''O_2$ complexes are more tightly bound and, therefore, more stable than $(Ca, Mg)_{1/2}Fe'''O_2$ complexes. Monovalent cations such as Li^+ and Na^+ may be incorporated in the pyroxene structure together with trivalent cations like Fe‴ in the form of the isomorphous phases $LiFe'''Si_2O_6$ and $NaFe'''Si_2O_6$. The role of isomorphous substitution of lithium in the pyroxene structure was not studied in detail. Lithium-containing pyroxenes are very rare in nature. Lithium iron pyroxene was described by Salman and coworkers[7,20,21] as $LiFe'''Si_2O_6$ among

the crystallization products of lithium silicate, lithium borosilicate and calcium lithium magnesium silicate with addition of iron oxide.

Glass G_1 has Li_2O/Al_2O_3 and CaO/MgO molar ratios equal to unity. Therefore, the Al_2O_3 and CaO are present in just enough amounts to combine with the corresponding Li_2O and MgO, respectively, in such silicate glasses to form β-spodumene ($LiAlSi_2O_6$) and diopside ($CaMgSi_2O_6$) phases:

$$Li_2O + Al_2O_3 + 4SiO_2 \rightarrow 2LiAlSi_2O_6$$
$$CaO + MgO + 2SiO_2 \rightarrow CaMgSi_2O_6$$

The crystallization of the glasses of low iron oxide content (i.e. 1 and 2 mol% Fe_2O_3, G_2 and G_3) generally developed pyroxene ss phases of diopsidic nature together with the lithia alumina bearing phases (β-eucryptite or β-spodumene). The X-ray analysis of both glasses crystallized at 950°C detected the *d*-spacing lines which were very similar to that of diopside. Segnit[22] determined the limits of solubility of iron as 10% in the $CaMgSi_2O_6$–Fe_2O_3 system, and concluded that half of the quantity of Fe‴ must replace silica in the tetrahedral position. The increase of intensities of the *d*-spacing with a slight shift of the diopside line with increasing Fe_2O_3/Al_2O_3 replacement may support the suggestion that iron oxide was accommodated in the diopside structure. Actually the two glasses had a Li_2O/Al_2O_3 ratio greater than unity (i.e. 1.16 and 1.40), i.e. there is an excess of Li_2O over that required to combine with Al_2O_3 to form the spodumene phase. Therefore, in the presence of iron oxide, it seems that the excess Li_2O can combine with iron oxide and silica to form alkali iron silicate:

$$Li_2O + Fe_2O_3 + 4SiO_2 \rightarrow 2LiFeSi_2O_6$$

$LiFeSi_2O_6$ is a new variety of clinopyroxene.[20] It seems, therefore, likely that during the crystallization of the glasses all the components of $LiFeSi_2O_6$ are accommodated in the diopside structure, where, in the presence of such a structure as a host crystal lattice which has a single chain structure, it is assumed that the Li and Fe‴ in eight-fold and six-fold coordination replace Ca and Mg respectively. This is supported by previous work on the $CaMgSi_2O_6$–$LiFeSi_2O_6$ glass system[7] which indicated that diopside can accommodate considerable amounts of $LiFeSi_2O_6$ in its structure forming a series of pyroxene solid solutions. Therefore the resulting pyroxene solid solution formed in G_2 and G_3 probably had the formula $(Ca_{0.88}Mg_{0.12})(Mg_{0.76}Fe_{0.12}Li_{0.12})Si_2O_6$ and $(Ca_{0.78}Mg_{0.22})(Mg_{0.56}Fe_{0.22}Li_{0.22})Si_2O_6$, respectively.

Further replacement of Al_2O_3 by Fe_2O_3 led to an increase of the pyroxene formation, a decrease of lithium aluminosilicate and consequently an increase in the Li_2O over Al_2O_3 required for spodumene formation. Therefore, in the case of G_4 and G_5 (with 3 and 4 mol% Fe_2O_3, respectively), the *d*-spacing lines of hedenbergite magnesium-like phase were only recorded together with spodumene and/or β-eucryptite. The diopside–hedenbergite minerals form a complete solid solution series between $CaMgSi_2O_6$ and $CaFe''Si_2O_6$. Most of the minerals of this series, however, contain other ions. In general, diopside–hedenbergite minerals of igneous rocks contain some ions replacing Ca, Mg and Fe″.[15] Hedenbergite is stable below 965°C and when heated at higher temperature it inverts to a homogeneous solid-solution phase of the same composition. The component of the $LiFeSi_2O_6$ phase seems to be incorporated in the pyroxene structure, giving rise to the probable pyroxene formula for G_4 and G_5 as $(Ca_{0.71}Mg_{0.29})(Mg_{0.42}Fe_{0.29}Li_{0.29})Si_2O_6$ and $(Ca_{0.59}Mg_{0.41})(Mg_{0.18}Fe_{0.41}Li_{0.41})Si_2O_6$, respectively.

At higher Al_2O_3/Fe_2O_3 replacement (i.e. 6 mol%, G_6) predominantly pyroxene solid-solution phase of augite nature and a lesser amount of β-eucryptite were formed. The resulting pyroxene solid-solution phase probably had the formula $(Ca_{0.27}Mg_{0.27}Fe_{0.23}Li_{0.23})SiO_3$. A very small amount of Li_2SiO_3 and iron oxide (Fe_2O_3) also appeared, especially at high temperature (800°C), as indicated by the X-ray analysis. Therefore, it is thought that a redistribution of the components of the glass takes place including partial dissociation of the $LiFeSi_2O_6$ component present in the augite pyroxene structure to the following components:

$$2LiFe'''Si_2O_6 \rightarrow Li_2SiO_3 + Fe_2O_3 + 3SiO_2$$

The residual silica in the equation may be incorporated in the lithium aluminosilicate forming β-eucryptite solid solution.

For the glass based on Li_2O–CaO–MgO–Fe_2O_3–SiO_2 (i.e. free of Al_2O_3; G_7), predominantly pyroxene solid solution of augite nature and α-quartz together with very small amounts of $Li_2Si_2O_5$, β-$LiFeO_2$ and iron oxide (Fe_2O_3) were detected. Augite and ferroaugite are the characteristic clinopyroxene phases and there is a continuous variation in their chemistry as well as in their optical properties. The structure of augite is similar to that of diopside. In this case a limited partial replacement of silica by Fe‴ ions seemed to be taking place in the tetrahedral position, which was accompanied by introducing Li^+ ions to preserve electrical neutrality, leading to the pyroxene formation of augite nature having the probable formula

$$(Ca_{0.33}Mg_{0.33}Li_{0.33})(Fe_{0.33}Si_{0.67})O_3.$$

The formation of considerable amounts of crystalline silica (as α-quartz) may support the suggestion that, during the crystallization, Fe‴

replaces silica in the formation of augite pyroxene phase. The formation of lithium disilicate, lithium ferrate and iron oxide may indicate also that a partial dissociation of $LiFeSi_2O_6$ component accommodated in the ferroaugite pyroxene structure takes place in the glass as follows:

$$3LiFeSi_2O_6 \rightarrow Li_2Si_2O_5 + LiFeO_2 + Fe_2O_3 + 4SiO_2$$

The fluctuation observed in the nature of the iron-containing phases formed in the present glasses might be thought to be connected with the state of iron in the glass and the change in iron coordination with its concentration in the glass.

5 Conclusion

A continuous iron pyroxene solid solution series can be formed in coloured glass-ceramics based on spodumene–diopside glass compositions with additions of Fe_2O_3 at the expense of Al_2O_3.

Iron oxide enhanced the formation of a fine-grained microstructure. It accelerates the β-eucryptite–β-spodumene transformation. However, it prefers to be accommodated in the pyroxene structure rather than in the lithium aluminosilicate phases. The characteristic *d*-spacings of iron pyroxene solid-solution phases vary with the gradual increase in iron oxide content in the glass from values of diopside–magnesium hedenbergite to those close to augite. Diopside can accommodate considerable amounts of $LiFeSi_2O_6$ components in its structure; in some cases, however (high Fe_2O_3/Al_2O_3 ratio), a partial dissociation of the latter component takes place in the glass and the phases like $Li_2Si_2O_5$, Li_2SiO_3, $LiFeO_2$, iron oxide and crystallized silica can result. These are greatly dependent upon the state and change of iron coordination with its concentration in the glass.

References

1. Brawer, S. A. & White, W. B., Structure and crystallization behaviour of Li_2O–Fe_2O_3–SiO_2 glasses. *J. Mat. Sci.*, **13** (1978) 1907–20.
2. Weaver, E. A. & Field, M. B., Magnetic, electrical and physical properties of Li_2O–Fe_2O_3–SiO_2 compositions. *Amer. Ceram. Soc. Bull.*, **52**(5) (1973) 467–72.
3. Rogers, P. S., The initiation of crystal growth in glasses. *Mineral. Mag.*, **37**(291) (1970) 741–58.
4. Beall, G. H., *Design of Glass-Ceramics*, *Reviews of Solid State Science*, Vol. 3, Nos 3 and 4. World Scientific Publishing Company, NJ, USA, 1989, pp. 333–54.
5. Berezhnoi, A. I., *Glass-Ceramics and Photo-Sitalls*. Plenum Press, NY, 1970.
6. McMillan, P. W., *Glass-Ceramics*, 2nd edn. Academic Press, NY, 1979.
7. Salman, S. M. & Salama, S. N., Pyroxene solid solutions crystallized from CaO–MgO(Li_2O, Fe_2O_3)–SiO_2 glasses. *Ceram. Int.*, **12** (1986) 221–8.
8. Williamson, J., Tipple, A. J. & Rogers, P. S., Influence of iron oxides on kinetics of crystal growth in CaO–MgO–Al_2O_3–SiO_2 glasses. *J. Iron Steel Inst.*, **206**(9) (1968) 898–903.
9. Rogers, P. S. & Williamson, J., The nucleation of crystalline phases in silicate glasses containing iron oxide. *Glass Technol.*, **10**(5) (1969) 128–33.
10. Kurkjian, C. R. & Sigety, E. A., Coordination of Fe^{3+} in glass. *Phys. Chem. Glasses*, **9**(3) (1968) 73–83.
11. Wang, M. L., Stevens, R. & Knott, P., Effects of microstructure on the colour variation of transparent glass ceramics. *Glass Technol.*, **23**(3) (1982) 139–45.
12. Ray, R. & Muchaw, G. M., High quartz solid solution phases from thermally crystallized glasses of composition (Li_2O–MgO) $Al_2O_3 n SiO_2$. *J. Amer. Ceram. Soc.*, **51**(12) (1968) 678–82.
13. Beall, G. H., Karstetter, B. R. & Rittler, H. I., Crystallization and chemical strengthening of stuffed β-quartz glass-ceramics. *J. Amer. Ceram. Soc.*, **50**(4) (1967) 181–90.
14. Kalinina, A. M. & Filipovich, V. N., The structure of glass: The sequence of crystallization on heating lithium aluminosilicate glasses, Vol. 5, ed. N. A. Toropov & E. A. Porai-Koshits. Consultants Bureau, New York, 1965, pp. 105–13.
15. Deer, W. A., Howie, R. A. & Zussman, J., *Rock Forming Minerals*, Vol. 2. Longman, London, 1963.
16. Hess, H. H., Chemical composition and optical properties of common clinopyroxenes. Part 1. *Amer. Mineral.*, **34** (1949) 621–9.
17. Salman, S. M., Thermal expansion characteristics of some iron-containing glasses and their corresponding crystalline materials. *Therm. Chim. Acta*, **81** (1984) 125–37.
18. Bishay, A. M., Colour and magnetic properties of iron in glasses of various types and their implications concerning structure: 1—high alkali silicate glasses. *J. Amer. Ceram. Soc.*, **42**(9) (1959) 403–7.
19. Waff, H. S., The structural role of ferric iron in silicate melts, *Canadian Mineral.* **15** (1977) 198–9.
20. Salman, S. M., Crystallization of alkali iron pyroxene $LiFeSi_2O_6$ in Li_2O–SiO_2 glasses containing iron oxide. *Interceram.*, **30**(1) (1981) 48–51.
21. Salman, S. M. & Mostafa, F., Crystallization of alkali iron borosilicate glasses. *Sprechsaal*, **18**(8) (1985) 672–9.
22. Segnit, E. R., Some data on synthetic aluminous and other pyroxenes, *Mineral Mag.*, **30** (1953) 218–23.